

---

# Parametric PET Imaging of 5HT<sub>2A</sub> Receptor Distribution with <sup>18</sup>F-Setoperone in the Normal Human Neocortex

Marie-Christine Petit-Taboué, Brigitte Landeau, Louisa Barré, Marie-Christine Onfroy, Marie-Hermine Noël and Jean-Claude Baron

INSERM U320, Cycleron, University of Caen, CEA DSV/DRM, Caen, France

---

Because of 5HT<sub>2A</sub> receptor's (5HT<sub>2A</sub>R) putative role in several neuropsychiatric diseases, studying it in vivo is an important goal. <sup>18</sup>F-setoperone is a well-validated and widely used PET radioligand for the study of neocortical 5HT<sub>2A</sub>R. We have previously developed and validated in baboons a method to generate parametric maps of the binding potential (i.e., the  $k_3$ -to- $k_4$  ratio) on a pixel-by-pixel basis, based on a single-dose tracer amount dynamic <sup>18</sup>F-setoperone PET paradigm, and with the receptor-poor cerebellum as reference structure. However, previous semiquantitative PET human studies suggested that nonspecific (NS) binding in the neocortex might not be identical to that in the cerebellum. **Methods:** As a first step in the development of  $k_3$ - $k_4$  parametric mapping in humans, we therefore estimated directly the NS binding of <sup>18</sup>F-setoperone in the neocortex of four young healthy volunteers who were studied with PET both before and after 2 wk of daily therapeutic oral doses of sertindole, an atypical neuroleptic possessing strong 5HT<sub>2A</sub>R antagonistic activity. **Results:** Visual analysis of the dynamic PET data obtained over 120 min confirmed that virtually full receptor saturation had indeed been achieved; however, the late neocortical time-activity curves (TACs) progressively fell to lower uptake values than corresponding cerebellar TACs and could not be fitted according to a four-compartment (four-Cpt) nonlinear model, indicating lack of specific binding. The cerebellum TACs for both the control and the challenge conditions, as well as the challenge neocortical TACs, were fitted according to three-Cpt modeling, providing the  $k_3/k_4$  ratio and in turn the  $f_2$  fraction for both structures. Despite the small sample of only four subjects, the  $f_2$  fraction for the neocortex was significantly larger (i.e., NS binding was smaller) than that estimated for the cerebellum. This allowed us to determine the  $k_3$ -to- $k_4$  ratio for the control neocortex using the challenge neocortex as reference structure, that is, without using the cerebellum at all. This "assumption-free" approach was also successfully used to generate  $k_3$ - $k_4$  maps for these four subjects, which showed highest values for the temporal cortex. **Conclusion:** This study shows that, for every new PET or SPECT radioligand and when estimation of specific binding is based on a reference structure, it is important to determine the uniformity of nonspecific binding before proceeding with human investigations.

**Key Words:** PET; serotonin; modeling; nonspecific binding  
**J Nucl Med 1999; 40:25–32**

---

**P**ET imaging of the 5HT<sub>2A</sub> receptor (5HT<sub>2A</sub>R) is of considerable interest both in pathophysiological (1–3), and psychopharmacological (4) investigations. One major advance in neuroreceptor PET studies is the generation of parametric maps of receptor distribution on a pixel-by-pixel basis (5), because it provides optimal quantitation and allows a comprehensive and objective brain volume analysis (6). Although it also has some affinity for the D<sub>2</sub> and 5HT<sub>2c</sub> receptors, <sup>18</sup>F-setoperone is a validated and widely used reversible PET radioligand for the study of the neocortical 5HT<sub>2A</sub>R (2,7–12); its distinct advantages are that its labeled metabolites do not cross the blood-brain barrier to any substantial degree (13) and that the cerebellum provides an adequate reference structure (see later discussion).

We have previously demonstrated in extensive baboon experiments (14) that <sup>18</sup>F-setoperone single-experiment metabolite-corrected kinetic PET data analysis allows quantitation of the binding potential (i.e., the  $k_3$ -to- $k_4$  ratio) of the neocortical 5HT<sub>2A</sub>R through the use of a novel multicompartmental modeling approach based on nonlinear three-compartment (three-Cpt) fitting of the cerebellum (Cb) data followed by four-Cpt graphical Logan-Patlak analysis of neocortex (NCx) data. Parametric images of the  $k_3$ -to- $k_4$  ratio on a pixel-by-pixel basis were subsequently obtained, which showed a regional distribution well correlated to in vitro 5HT<sub>2A</sub>R density data (14). The Cb, a structure virtually devoid of 5HT<sub>2A</sub>R, has been used in all the aforementioned investigations to estimate the free and the nonspecific (NS) binding in the neocortex. This approach is based on studies in the baboon (7) that showed not only that presaturation with a 5HT<sub>2A</sub>R blocker did not affect the cerebellar <sup>18</sup>F-setoperone kinetics (confirming the lack of displaceable specific binding there) but also that the neocortical kinetics became superimposed onto those of the Cb, suggesting similar NS components in the two structures. We have recently validated this in the baboon by means of formal compartmental modeling, showing no significant difference in the  $f_2$  fraction (i.e.,  $[1 / (1 + k_3/k_4)]$ , an index of NS) between Cb and NCx (15). However, formal documentation of uniform NS binding of <sup>18</sup>F-setoperone in NCx and Cb in

---

Received Apr. 1, 1998; accepted May 20, 1998.

For correspondence or reprints contact: Jean-Claude Baron, MD, INSERM U320-Cycleron, BP 5229, Bd Becquerel, 14074 Caen, France.

the human species is still lacking, presumably because presaturation studies in humans are seldom possible because of the risk of pharmacological effects (16). In the single validation study, which used chronic oral treatment by ketanserin, only two patients were reported on (8) and the results provided equivocal evidence for uniform NS binding.

We have reevaluated this issue in a small group of healthy subjects in whom we directly estimated and compared the  $f_2$  fraction in the NCx and the Cb from formal modeling of saturation kinetic PET data. Because we also obtained tracer-only  $^{18}\text{F}$ -setoperone kinetic data in the same subjects, it was possible to derive for the first time in humans values for NCx  $^{18}\text{F}$ -setoperone binding potential that made no assumption about the validity of the Cb as reference structure. That is to say, it became possible to incorporate the  $K_1$ ,  $k_2$ ,  $k_5$  and  $k_6$  values obtained from NCx data fitting in the saturation condition into the fitting of the tracer-only NCx data and, in turn, to derive directly the  $k_3$ -to- $k_4$  ratio. We applied this approach to whole NCx data and also on a pixel-by-pixel basis to obtain, in this small group of healthy subjects, parametric maps of such assumption-free binding potential. This work was presented as a poster and abstract at the 1997 Annual Meeting of the Society of Nuclear Medicine (17).

## MATERIALS AND METHODS

### PET Experiments

**Radiochemistry.**  $^{18}\text{F}$ -setoperone was synthesized using the method described by Crouzel et al. (18). Setoperone was labeled by nucleophilic substitution of an  $\text{N}_2\text{O}$  group by  $^{18}\text{F}$ . Reactivity of  $^{18}\text{F}$  was increased with Kriptofix 2.2.2. (Sigma-Aldrich, Lyons, France) and  $\text{K}_2\text{CO}_3$ . After evaporation,  $\text{K}^{18}\text{F}$  reacted with a nitro derivative of setoperone. The product was purified by high-performance liquid chromatography (HPLC).

**Subjects and Design.** After giving written informed consent, four young healthy men (age  $30.5 \pm 5$  y) were studied by PET with  $^{18}\text{F}$ -setoperone before (control) and after (challenge) 14 d of daily oral treatment with therapeutic doses of sertindole, an atypical neuroleptic of the fluoro-phenyl-indole family that possesses strong  $5\text{HT}_{2A}\text{R}$  antagonist activity ( $K_i = 0.2$  nM), such that at the doses and regimen used (4 mg three times a day, orally), substantial, and perhaps even full, occupancy of the neocortical  $5\text{HT}_{2A}\text{R}$  would be expected (19,20).

Three-dimensional T1-weighted MRI (SPGR sequence, 128 adjacent cuts) was performed in each subject using a 1.5-T, General Electric (Buc, France) device.

After establishing the presence of satisfactory collateral circulation, we inserted a thin radial catheter into the radial artery under xylocaine local anesthesia. In both PET examinations, tracer amounts of  $^{18}\text{F}$ -setoperone at high specific radioactivity ( $\text{SRA} = 3.92 \pm 1.02$  Ci/ $\mu\text{mol}$ , mean  $\pm$  SD) were injected intravenously as a bolus ( $6.73$  mCi  $\pm$  0.93, mean  $\pm$  SD, for the eight studies).

**PET Data Acquisition.** PET data were acquired with the seven-slice LETI TTV03 time-of-flight camera (intrinsic resolution:  $5.5 \times 5.5 \times 9$  mm, x,y,z) (LETI, Grenoble, France). The positioning and movement of the patient's head were controlled and prevented by the use of Laitinen's stereotactic frame (Issal

Surgical Instruments, Stockholm, Sweden). Using a method based on a lateral skull radiograph and derived from that of Fox et al. (21), we positioned the subjects with reference and parallel to the glabella-inion (GI) line. Thus, we obtained seven PET planes from GI -4 mm to GI +68 mm. After a transmission scan with  $^{68}\text{Ge}$ , the PET acquisition with list mode procedure started from the beginning of the bolus injection ( $T_0$ ) and lasted 120 min. Data were reconstructed with the following image frame sequences:  $9 \times 16$  s,  $5 \times 30$  s,  $5 \times 60$  s,  $6 \times 300$  s and  $4 \times 1200$  s. Initial (0-2 min) 2-s head counts were also recorded (22) to fit the brain-to-arterial shift of  $^{18}\text{F}$ -setoperone rise (23). The PET data were automatically corrected for  $^{18}\text{F}$  decay, and scatter was empirically corrected based on the technique of Bendriem et al. (24).

**Quantification of Arterial Radioactivity and  $^{18}\text{F}$ -Labeled Metabolites.** Arterial sampling started simultaneously with PET acquisition at the start of radiotracer injection; about 12 samples ( $\sim 1$  mL) were withdrawn in the first minute and about 10 samples ( $\sim 1$  mL) were withdrawn at increasing intervals until the end of the study. Radioactivity in whole blood and total plasma, corrected for  $^{18}\text{F}$  decay, were measured in units of nanocurie per milliliter by a gamma counter (Packard, Rungis, France) cross-calibrated with the PET camera.

Plasma input function was corrected for the presence of  $^{18}\text{F}$  metabolites (13,14) as estimated by thin-layer radiochromatography (TLRC). Briefly, plasma was deproteinated with methanol. After evaporation of the supernatant, the residue was dissolved in a mixture of acetonitrile and methanol and was analyzed by TLRC with dichloromethane/methanol/ethylamine (100:12:0.2 vol) as the migration solvent. This allowed us to express the results in terms of percentage of unchanged  $^{18}\text{F}$ -setoperone for each determination. The plasma  $^{18}\text{F}$  time-course for each subject was corrected for the measured fraction of metabolites. Arterial whole-blood  $^{18}\text{F}$  curves were used to determine the vascular fraction.

**Image Handling and Regions of Interest.** For each subject, the two sets of PET data and the coregistered MRI volume were realigned in three dimensions using the method of Woods et al. (25). Neocortical ( $n = 90$ ) and cerebellar ( $n = 5$ ) circular regions of interest (ROIs; 14-mm diameter) were anatomically defined onto the individual MR image of each subject and were resliced according to the seven PET planes with the help of Talairach and Tournoux's stereotactic atlas of the human brain (26). To obtain time-activity curves (TACs), radioactivity concentration in these regions (weighted mean of all voxels in each region) was calculated for each sequential scan and was plotted versus time using dedicated software (MIRIAM).

To generate whole-neocortex (Whole-NCx) TACs in which to estimate the neocortical NS fraction and binding potential, all the pixel data contained in the 90 neocortical ROIs were averaged. In addition, we obtained TACs for Cb and for the different neocortical lobes by averaging the original ROI values from different PET planes into mean lobes, such as frontal, temporal, parietal and occipital, according to Marchal et al. (27).

### Estimation of the NS Fraction

Apparently full saturation of the  $5\text{HT}_{2A}$  was obtained in each of the four subjects (Fig. 1), which allowed us to proceed with the determination of the NS fraction in the NCx as follows: The Cb control and challenge TACs as well as the challenge Whole-NCx data were fitted according to a three-Cpt model (i.e., with  $k_3:k_4$  equal to 0) with standard nonlinear least-squares (NLSQ) method (14). This allowed us to evaluate directly  $K_1$ ,  $k_2$ ,  $k_5$  and  $k_6$

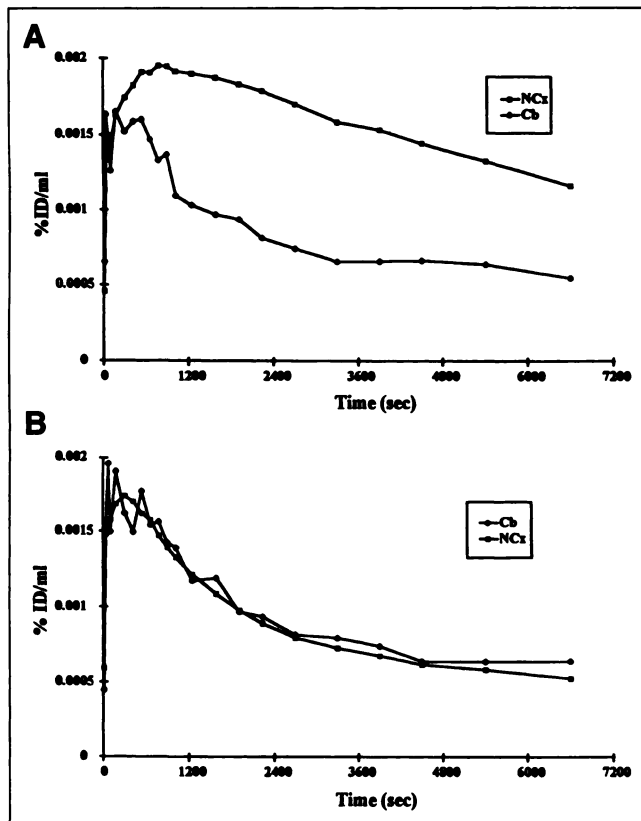


**FIGURE 1.** Time-activity curves obtained for subject 3 in control (A) and in challenge (B) cerebellum and whole neocortex, expressed in percent of injected dose per milliliter tissue (%ID/mL), after injection of  $^{18}\text{F}$ -setoperone.

and the  $f_2$  fraction for both the Cb (each condition) and the NCx, because  $f_2 = [1 / (1 + k_5/k_6)]$ .

### General Modeling Strategy

The binding potential from the control Whole-NCx TACs was estimated according to our previously described original method (method 2 of Petit-Taboué et al., 14), with the only difference being that the Cb was replaced by the challenge Whole-NCx as reference for  $K_1$ ,  $k_2$ ,  $k_5$  and  $k_6$ . To do this, the challenge and control Whole-NCx TACs were fitted according to a three-Cpt and a four-Cpt model, respectively, using a general model where the rate constants are  $K_1$  (mL/g  $\times$  min) and  $k_2$  for transport into and out of free ligand compartment,  $k_3$  and  $k_4$  for binding to and dissociation from the  $5\text{HT}_{2A}\text{R}$  and  $k_5$  and  $k_6$  for binding to and dissociation from NS compartment ( $k_2$ - $k_6$ ,  $\text{min}^{-1}$ ). The initial fitting values were those previously defined in baboon studies (14). The neocortical binding potential was calculated as  $k_3:k_4$  (16).  $V_f$  represents the vascular fraction in the ROI and was allowed to vary in the model. Method 2 of Petit-Taboué et al. (14) is based on a four-Cpt Logan-Patlak graphical analysis (28), where the slope of the plot is given by  $[K_1/k_2 (1 + k_3/k_4 + k_5/k_6)]$  (14). Thus, with a prior three-Cpt NLSQ procedure on the Whole-NCx<sub>challenge</sub> data to estimate  $K_1:k_2$  and  $k_5:k_6$ , we were able to directly determine the  $k_3$ -to- $k_4$  ratio (14). The equation used in the graphical analysis of reversible systems (28) is given by:

$$\frac{\int_0^T \text{ROI}(t) dt}{\text{ROI}(T)} = a \frac{\int_0^T C_p(t) dt}{\text{ROI}(T)} + b,$$

where  $\text{ROI}(t)$  is the radioactivity measured at time  $t$  and  $C_p(t)$  is the plasma radioactivity due to the unmetabolized ligand. When a state of pseudoequilibrium is reached, the plot becomes linear.

### Parametric Images of $k_3:k_4$

Using the same equation as in the previous analysis, the neocortical binding potential was also assessed on a pixel-by-pixel basis. To do this, the aforementioned graphical analysis was applied on the final six data points, providing a slope for each pixel. All pixels with negative slopes were set to 0, and the quality of the fit for the retained pixels was ensured by checking all the correlation coefficients for their closeness to 1. Using the  $K_1$ ,  $k_2$ ,  $k_5$  and  $k_6$  transfer coefficients determined from the Whole-NCx<sub>challenge</sub> according to the ROI analysis (see earlier discussion), we then computed the  $k_3$ -to- $k_4$  ratio for each pixel of the seven PET planes in each subject. Before applying  $k_5:k_6$  from the Whole-NCx<sub>challenge</sub>, however, we checked that no systematic difference in  $k_5:k_6$  values occurred between the different cerebral lobes, based on three-Cpt modeling of TACs obtained in the challenge condition.

## RESULTS

### Determination of the NS Fraction

**TACs.** Both the cerebellar and the neocortical TACs in all four control studies showed typical profiles of  $^{18}\text{F}$ -setoperone kinetics with rapid uptake in both Cb and Whole-NCx but with rapid washout from the former and slower washout from the latter. In the challenge condition, no effect of treatment was observed on the Cb TACs, as expected from the earlier studies of Blin et al. (8), but in each subject the neocortical  $^{18}\text{F}$  time course progressively fell below that of the Cb, suggesting full inhibition of specific binding with lower residual binding (i.e., lower NS binding) in the NCx. This is illustrated in Figure 2.

**Fitting Results.** Both the Cb<sub>control</sub> TACs and the Cb<sub>challenge</sub> TACs were modeled according either to a two-Cpt or to a three-Cpt model (Fig. 3). As clearly illustrated by both the visual result of the fits and the significant decrease of the Akaike Information Criteria (AIC values  $147 \pm 36$  and  $79 \pm 9$ , respectively,  $P < 0.05$ ), the fit on Cb<sub>control</sub> TACs was consistently better with the three-Cpt than with the two-Cpt model. This finding indicates that, as was the case in the baboon (14), the free and NS compartments for  $^{18}\text{F}$ -setoperone in the human Cb may not be in rapid equilibrium and thus need to be kinetically separated with a three-Cpt model. The same findings also applied to the Cb<sub>challenge</sub> (AIC values  $145 \pm 36$  and  $72 \pm 8$ , respectively,  $P < 0.05$ ). Neither the rate constants (Table 1) nor the  $f_2$  fraction significantly differed between the control and the challenge studies ( $0.427 \pm 0.140$  and  $0.493 \pm 0.047$ , respectively,  $P > 0.05$ ).

The Whole-NCx<sub>challenge</sub> TACs could be fitted only according to a three-Cpt model (i.e., with  $k_3:k_4$  equal to 0), whereas a four-Cpt model failed to fit the data, confirming that virtually full  $5\text{HT}_{2A}\text{R}$  saturation (i.e., without specific binding component) was indeed achieved in these circumstances. The fitting results therefore provided directly the transfer coefficients  $K_1$ ,  $k_2$ ,  $k_5$  and  $k_6$  and, in turn, the  $f_2$  fraction for the NCx. The individual and mean ( $\pm$ SD) estimates of the transfer coefficients are presented in Table 2. Although the  $k_5$

## <sup>18</sup>F - Setoperone

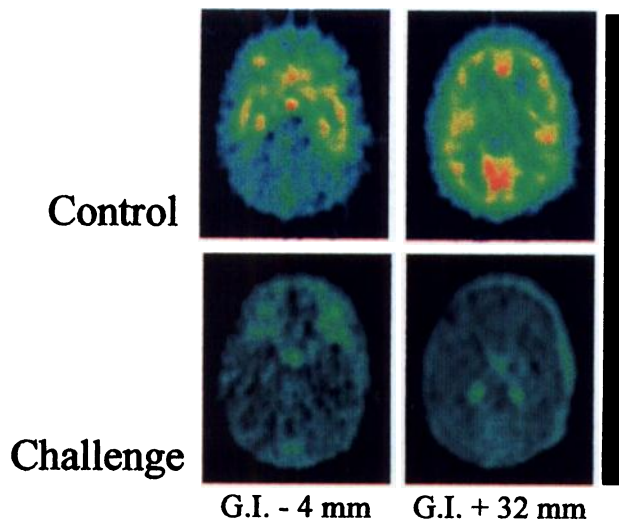


**FIGURE 2.** PET images of <sup>18</sup>F-setoperone uptake accumulated between 60 and 120 min after radioligand injection, obtained in same subject in control (untreated) condition, and 2 wk after oral treatment with pharmacologic doses of atypical neuroleptic (challenge). Two levels are shown relative to glabella-inion (GI) line to illustrate plane through cerebellum (left) and neocortex (right). These images illustrate high uptake in neocortex with low uptake in cerebellum in control condition, consistent with known distribution of 5HT<sub>2A</sub>R, but markedly reduced neocortical uptake in challenge condition, indicating near saturation of 5HT<sub>2A</sub>R.

for Cb was higher than for NCx, no difference between any of these values and those obtained by three-Cpt modeling on the Cb<sub>challenge</sub> data reached statistical significance.

The values for the  $f_2$  fraction (calculated as  $[1/(1 + k_5:k_6)]$ ) are shown in Table 3. In each of the four subjects, the  $f_2$  value for the NCx was higher than the corresponding value obtained for the Cb, with a significant difference between the two structures across the group (Table 3).

The volume of distribution (i.e.,  $K_1:k_2$ ) in the challenge condition did not significantly differ between the NCx and the Cb and was similar to that found for the latter structure in the control condition (Tables 1 and 2).

### Whole-NCx ROI Analysis

In all four cases, visual analyses of the Logan-Patlak plots or Whole-NCx<sub>control</sub> TACS showed clear-cut linearity after the expected early bend, with linearity beginning for times > 10 min (Fig. 2D). The slopes were automatically determined by linear regression on all values for  $t > 10$  min. As expected, the slopes were significantly greater for Whole-NCx<sub>control</sub> than for Whole-NCx<sub>challenge</sub> ( $9.87 \pm 1.2$  and  $3.97 \pm 0.15$ , respectively,  $P < 0.01$ ). The  $k_3$ -to- $k_4$  ratios obtained according to this graphical method combined with three-Cpt NLSQ on Whole-NCx<sub>challenge</sub> data are shown in Table 2.

### Parametric Images of the $k_3:k_4$ Ratio

To assess uniformity of the  $f_2$  value across the different cortical areas, we fitted the TACs for the four cerebral lobes

from the challenge condition with a three-Cpt model; the results showed no significant difference among the four lobes ( $f_2 = 0.583 \pm 0.036$ ,  $0.481 \pm 0.62$ ,  $0.515 \pm 0.112$  and  $0.510 \pm 0.159$ , for the frontal, occipital, parietal and temporal lobes, respectively;  $P = 0.62$  by repeated-measures analysis of variance), which allowed us to use the Whole-NCx  $f_2$  value to generate parametric maps of  $k_3:k_4$ . These maps demonstrated high levels of binding in frontal, temporal, parietal and occipital areas as compared to other parts of the brain. An example is shown in Figure 4. Presented in Table 4 are the individual and mean ( $\pm$ SD)  $k_3:k_4$  values in the different cortical lobes, suggesting highest binding potential for the temporal cortex.

### DISCUSSION

This study showed that, at variance with the baboon, the NS fraction was significantly lower in the NCx than in the Cb in these subjects. This in turn allowed us for the first time to calculate the binding potential for neocortical ROIs and to generate maps of  $k_3:k_4$  for <sup>18</sup>F-setoperone in humans, without making any assumption as to the validity of the Cb as a reference structure. Our results also confirm the validity of our modeling approach developed first in the nonhuman primate (14) to quantify in vivo <sup>18</sup>F-setoperone specific binding to the 5HT<sub>2A</sub>R with single-dose kinetic PET experiment. Our modeling approach was previously extended only in part to human studies (9,29).

In all previous human and baboon experiments, the Cb served as a reference structure to estimate the NS binding of <sup>18</sup>F-setoperone in the NCx with NLSQ fitting, Patlak-Logan graphical analysis or simple pseudo-equilibrium (i.e., NCx:Cb ratio) approaches (9–11,14). Previous semiquantitative studies of the kinetics of <sup>18</sup>F-setoperone in the baboon Cb suggested a lack of specific binding in this structure, as indicated by pretreatment studies with spiperone or ketanserin (7). We have recently confirmed this according to formal compartmental modeling in this species (15) and have found that the neocortical  $f_2$  fraction estimated after blocking of the 5HT<sub>2A</sub>R with cold setoperone was not significantly different from that found in the Cb. Thus, the use of the Cb as a reference structure to estimate the neocortical F and NS components of <sup>18</sup>F-setoperone is valid in the baboon. These findings indicate, however, that in humans, the NS is significantly lower in the NCx than in the Cb. Although the study sample was small, the findings of larger  $f_2$  in NCx than in the Cb was consistent across all four subjects and was statistically significant, suggesting that the results are reliable. Previously, only two studies have reported <sup>18</sup>F-setoperone kinetics in the NCx and the Cb in subjects treated with 5HT<sub>2A</sub> blockers. Blin et al. (8) reported on two subjects chronically treated with oral ketanserin (80 mg/d), a potent 5HT<sub>2A</sub> blocker; the data shown in Figure 4B of their article indicate lower late (from 70 min onward)

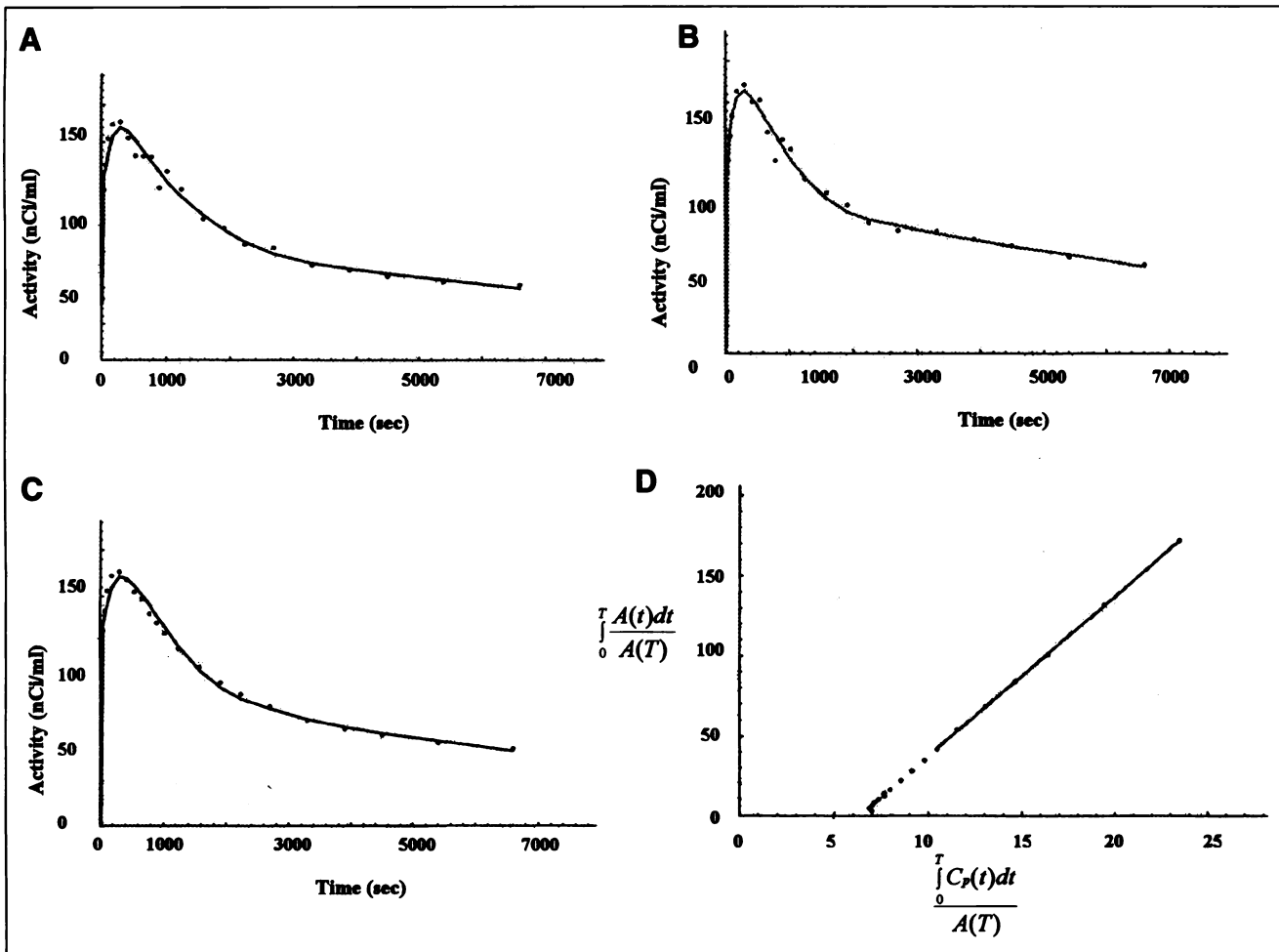


**FIGURE 3.** Illustrative NLSQ fitting procedure from one subject. Three-compartment NLSQ fit on (A) cerebellar control data, (B) cerebellar challenge data and (C) neocortical challenge data from same subject as Figure 1 (the data are expressed in nanocuries per milliliter in this graph; injected amounts of  $^{18}\text{F}$ -setoperone in this subject were 6.71 mCi and 7.59 mCi in control and challenge conditions, respectively). (D) Logan-Patlak plot with linear fit for  $t > 10$  min of corresponding neocortical control data.

$^{18}\text{F}$ -setoperone uptake in the NCx than in the Cb, consistent with our findings. Fischman et al. (9) studied eight subjects who were given a single oral dose of ziprasidone (40 mg), an atypical neuroleptic with  $5\text{HT}_{2\text{A}}$  and  $\text{D}_2$  blocking activity. The brain  $^{18}\text{F}$ -setoperone kinetics were studied with PET for

90 min after radiotracer injection and at different times after dosing with ziprasidone (i.e., two subjects each at 4, 8, 12 and 24 h after drug administration). The data shown in Figure 3B of their article for the earliest time after dosing (i.e., 4 h) suggest superimposable NCx and Cb kinetics up to

**TABLE 1**  
Individual and Mean ( $\pm$ SD) Estimates of Transfer Coefficients ( $K_1$  and  $k_2-k_6$ ) and Vascular Fraction ( $V_f$ ) and Ratio  $K_1$ -to- $k_2$  by NLSQ for Cerebellar (Control [ $\text{Cb}_{\text{control}}$ ] and Challenge [ $\text{Cb}_{\text{challenge}}$ ] Studies)  $^{18}\text{F}$ -Setoperone Time-Activity Data

Subject no.	$K_1$		$k_2$		$K_1:k_2$		$k_5$		$k_6$	
	$\text{Cb}_{\text{control}}$	$\text{Cb}_{\text{challenge}}$								
1	0.249	0.265	0.13	0.105	1.919	2.523	0.0188	0.0146	0.0254	0.0177
2	0.113	0.230	0.042	0.079	2.718	2.897	0.0080	0.0097	0.0029	0.0096
3	0.278	0.268	0.078	0.087	3.563	3.094	0.0178	0.0177	0.0186	0.0175
4	0.261	0.243	0.089	0.086	2.944	2.827	0.0120	0.0113	0.0065	0.0086
Mean	0.225	0.252	0.085	0.089	2.786	2.835	0.0141	0.0133	0.0133	0.0134
SD	0.076	0.018	0.036	0.011	0.679	0.237	0.0050	0.0035	0.0104	0.0049

There was no significant difference in the fitted values between the two conditions for any parameter.  
NLSQ = nonlinear least-squares procedure.

**TABLE 2**

Estimates of Transfer Coefficients ( $K_1$  and  $k_2-k_6$ ) and Vascular Fraction ( $V_f$ ) by Three-Compartment Nonlinear Least Squares for Whole-Neocortex (Challenge Studies)  $^{18}\text{F}$ -Setoperone Time-Activity Data and  $k_3$ -to- $k_4$  Ratio Estimated by Four-Compartment Logan-Patlak Graphical Analysis on Control Whole-Neocortex Data

Subject no.	Challenge studies						Control studies
	$K_1$	$k_2$	$K_1:k_2$	$k_5$	$k_6$	$V_f$	$k_3:k_4$
1	0.235	0.085	2.770	0.0120	0.0175	0.074	1.197
2	0.201	0.064	3.129	0.0047	0.0055	0.094	1.569
3	0.217	0.066	3.300	0.0069	0.0112	0.076	1.401
4	0.240	0.085	2.818	0.0117	0.0140	0.072	2.019
Mean	0.223	0.075	3.004	0.0088	0.0120	0.079	1.547
SD	0.018	0.012	0.254	0.0036	0.0051	0.010	0.350

NLSQ = nonlinear least-squares procedure.

90 min, and four-Cpt modeling resulted in a calculated  $5\text{HT}_{2A}\text{R}$  occupancy of 98%; data obtained at later times showed lower occupancies. Although our results are in apparent conflict with those reported by Fishman et al., several major differences between the two studies might explain this discrepancy. First, Fischman et al. (9) did not report data later than 90 min, compared to 120 min in this study and 110 min in Blin et al. (8). Second, Fischman et al. (9) used a single-dose regimen, whereas we and Blin et al. (8) used a chronic regimen more prone to induce full receptor occupancy. Third, the highest occupancy value calculated by Fischman et al. (9), estimated at 98%, was obtained by four-Cpt modeling that was possible on their NCx data, indicating residual specific binding, whereas four-Cpt modeling was impossible in our subjects. Overall, therefore, due to the chronic oral regimen, Blin et al. (8) and we were able to induce near complete receptor saturation, which in both cases showed lower nondisplaceable uptake in the NCx than in the Cb in humans.

Differences in NS fraction between the reference and the

**TABLE 3**

Individual and Mean ( $\pm$ SD) Estimates of the  $f_2$  Fraction for the Cerebellum and Whole-Neocortex Challenge Studies

Subject no.	$\text{Cb}_{\text{challenge}}$	$\text{NCx}_{\text{challenge}}$	Difference (NCx - Cb)
1	0.548	0.593	+0.045
2	0.496	0.540	+0.044
3	0.497	0.621	+0.124
4	0.432	0.547	+0.115
Mean	0.493	0.575	+0.082*
SD	0.047	0.039	0.043

$\text{Cb}_{\text{challenge}}$  and  $\text{NCx}_{\text{challenge}}$  = data from challenge cerebellar and whole-neocortical time-activity curves.

\*Significant difference by Student paired  $t$  test ( $t = 3.81$ ,  $df = 3$ ,  $P < 0.05$ ).

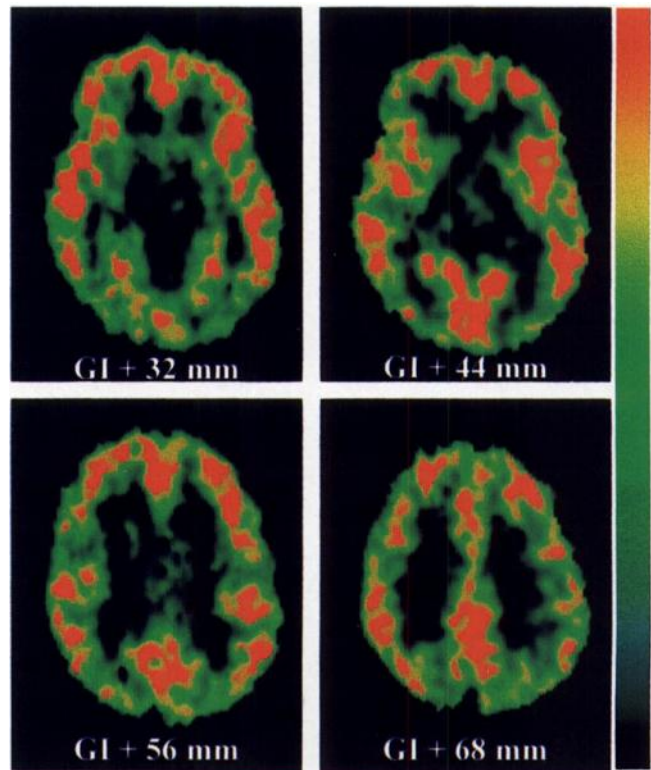


**FIGURE 4.** Parametric pixel-by-pixel images of the neocortical binding potential (Material and Methods section), illustrated for four PET levels above the GI line (GI +32, +44, +56 and +68 mm). This shows high binding potential (i.e.,  $k_3:k_4$ ) in entire neocortex, maximal in temporal regions (in red). See Table 4 for values obtained in specific neocortical ROIs. Note that, for display purposes, an eight-connexity smoothing filter was applied on raw parametric images, but ROI data were generated from unsmoothed images.

target structure have been suggested previously for both  $^{11}\text{C}$ -raclopride (30), with NS binding 35% higher in the striatum compared to the Cb, and  $^{18}\text{F}$ -fluoro-ethyl-spiperone (31), in which the use of the Cb as reference structure led to an underestimation of the rate constant  $k_3$  for the striatum. Lassen et al. (32) have shown that an overestimation of the NS fraction, as would have occurred here if the Cb was used as (uncorrected) reference, results in an underestimation of  $B_{\text{max}}/K_d$ . Thus, this issue should be considered for every new PET or SPECT radioligand, and challenge studies should be

**TABLE 4**

Individual Values and Mean ( $\pm$ SD) for  $^{18}\text{F}$ -Setoperone Binding Potential to the  $5\text{HT}_{2a}$  Receptor for the Different Cortical Lobes Obtained on Pixel-by-Pixel Basis

Subject no.	Frontal	Temporal	Parietal	Occipital
1	0.806	0.804	0.603	0.842
2	1.915	2.087	1.870	1.858
3	1.363	1.343	1.059	1.267
4	1.705	1.749	1.621	1.773
Mean	1.447	1.496	1.288	1.435
SD	0.484	0.552	0.569	0.474

performed even in a limited sample of subjects, whenever this is acceptable in terms of potential side effects.

The volume of distribution (i.e.,  $K_1:k_2$ ) was uniform between the Cb and the NCx and was not affected by treatment, reinforcing the robustness of our findings regarding  $f_2$ . The same results were obtained previously in baboons (15). With other ligands such as  $^{18}\text{F}$ -spiperone (33),  $^{11}\text{C}$ -carfentanyl (34) and  $^{11}\text{C}$ -diprenorphine (35), an increase of  $k_2$  without change of  $K_1$  was observed after presaturation.

In this study, we have successfully applied to human data our novel method previously validated in baboons, which uses a four-Cpt Logan-Patlak graphical analysis combined with three-Cpt NLSQ fitting of the reference TACs (i.e., method 2 of Petit-Taboué et al., 14), except we used the  $\text{NCx}_{\text{challenge}}$  as reference rather than the  $\text{Cb}_{\text{control}}$ . As in the baboon, the slopes obtained here for the control NCx became rapidly linear (for  $t > 10$  min). Another expected finding was a significant decrease in slopes of the Logan-Patlak plots with receptor occupancy, which confirms earlier suggestions by Sadzot et al. (36) that this graphical method is sensitive to receptor occupancy and could be used as a quantitative tool in these kinds of pharmacological investigations.

We also applied the same method on a pixel-by-pixel basis to generate parametric images of the binding potential. The images obtained were of good quality and appeared artifact-free, showing an essentially homogeneous distribution of the specific binding throughout the NCx (Fig. 4). However, highest binding potential was observed in the temporal cortex, which agrees well with in vitro  $^3\text{H}$ -ketanserin data (37,38).

## CONCLUSION

This study provides evidence for nonuniformity of NS binding of  $^{18}\text{F}$ -setoperone between the NCx and the Cb. Although this difference cannot at present be generalized to all age groups, both sexes or all disease conditions, it will have to be considered in future studies with this otherwise convenient and suitable radioligand.

## ACKNOWLEDGMENTS

We are grateful to the staff of the Biomedical Cyclotron and Radiochemistry Unit at Cyceron, and specifically to Meziane Ibazizene for metabolite quantitation and to Hervé Boutin for his help in the statistical analysis. Martine Huguet and Anita Foro helped with preparation of the article. We also thank Lundbeck Laboratoires (Copenhagen, Denmark) for allowing us to publish this material.

## REFERENCES

1. Mayberg HS, Parikh RM, Morris PL, Robinson RG. Spontaneous remission of post-stroke depression and temporal changes in cortical 5-HT<sub>2</sub>-serotonin receptors. *J Neuropsychiatry Clin Neurosci*. 1991;3:80-83.
2. Blin J, Baron JC, Dubois B, et al. Loss of brain 5-HT<sub>2</sub> receptors in Alzheimer's disease. *Brain*. 1993;116:497-510.
3. Vera P, Zilbovicius M, Chabriat H, et al. Post-stroke changes in cortical 5-HT<sub>2</sub> serotonergic receptors. *J Nucl Med*. 1996;37:1976-1981.
4. Nordström AL, Farde L, Halldin C. High 5-HT<sub>2</sub> receptor occupancy in clozapine treated patients demonstrated by PET. *Psychopharmacology*. 1993;110:365-367.
5. Blomqvist G, Lammertsma AA, Mazoyer B, Wienhard K. Effect of tissue heterogeneity on quantification in positron emission tomography. *Eur J Nucl Med*. 1995;22:652-663.
6. Richardson MP, Koepp MJ, Brooks DJ, Fisc DR, Duncan JS. Benzodiazepine receptors in focal epilepsy with cortical dysgenesis: an  $^{11}\text{C}$ -flumazenil PET study. *Ann Neurol*. 1996;40:188-198.
7. Blin J, Pappata S, Kiyosawa M, Crouzel C, Baron JC.  $^{18}\text{F}$ -setoperone: a new affinity ligand for positron emission tomography study of the serotonin-2 receptors in baboon brain in vivo. *Eur J Pharmacol*. 1988;147:73-82.
8. Blin J, Sette G, Fiorelli M, et al. A method for the in vivo investigation of the serotonergic 5-HT<sub>2</sub> receptors in the human cerebral cortex using positron emission tomography and  $^{18}\text{F}$ -labeled setoperone. *J Neurochem*. 1990;54:1744-1754.
9. Fischman AJ, Bonad AA, Babich JW, et al. Positron emission tomography analysis of central 5-hydroxytryptamine<sub>2</sub> receptor occupancy in healthy volunteers treated with the novel antipsychotic agent Ziprasidone. *J Pharmacol Exp Ther*. 1996;279:939-947.
10. Chabriat H, Tehindrazanarivelo A, Vera P, et al. 5HT<sub>2</sub> receptors in cerebral cortex of migraineurs studied using PET and  $^{18}\text{F}$ -fluorasetoperone. *Cephalalgia*. 1995;15:104-108.
11. Kapur S, Jones C, DaSilva J, Wilson A, Houle S. Reliability of a sample non-invasive method for the evaluation of 5-HT<sub>2</sub> receptors using [ $^{18}\text{F}$ ]-setoperone PET imaging. *Nucl Med Commun*. 1997;18:395-399.
12. Lewis R, Kapur S, Jones C, et al. PET study of 5-HT<sub>2</sub> receptor density in schizophrenia [Abstract]. *Biol Psychiatry*. 1997;41:63S.
13. Blin J, Crouzel C. Blood-cerebrospinal fluid and blood-brain barriers imaged by  $^{18}\text{F}$ -labeled metabolites of  $^{18}\text{F}$ -setoperone studied in humans using positron emission tomography. *J Neurochem*. 1992;58:2303-2310.
14. Petit-Taboué MC, Landeau B, Osmont A, Tillet I, Barré L, Baron JC. Estimation of neocortical serotonin-2 receptor binding potential by single-dose fluorine-18-setoperone kinetic PET data analysis. *J Nucl Med*. 1996;37:95-104.
15. Petit-Taboué MC, Landeau B, Young AR, et al. Estimation of non-specific binding of  $^{18}\text{F}$ -setoperone, a 5HT<sub>2A</sub>-receptor PET radioligand, from saturation kinetic data in the baboon and human neocortex. In: Daube-Witherspoon ME, Herscovitch P, eds. *Quantitative Functional Brain Imaging with Positron Emission Tomography*. San Diego, CA: Academic Press; 1998:415-420.
16. Mintun MA, Raichle ME, Kilbourn MR, Wooten GF, Welch MJ. A quantitative model for the in vivo assessment of drug binding sites with positron emission tomography. *Ann Neurol*. 1984;15:217-227.
17. Petit-Taboué MC, Landeau B, Young AR, et al. Estimation of non-specific (NS) binding of fluorine-18-setoperone (fluorine-18-set), a 5HT<sub>2</sub>-receptor ( $5\text{HT}_{2\text{A}}$ ) PET radioligand, in the baboon and human neocortex [Abstract]. *J Nucl Med*. 1997;38:200P.
18. Crouzel C, Venet M, Irie T, Sanz G, Boullais C. Labelling of serotonergic ligand with  $^{18}\text{F}$ - $^{18}\text{F}$ -setoperone. *J Label Comp Radiopharmacol*. 1988;25:403-414.
19. Van Kammen DP, McEvoy JP, Targum SD, Kardatzke D, Sebree TB. A randomized, controlled, dose-ranging trial of sertindole in patients with schizophrenia. *Psychopharmacology* 1996;124:168-175.
20. Zimbroff DL, Kane JM, Tamminga CA, et al. Controlled, dose-response study of sertindole and haloperidol in the treatment of schizophrenia. *Am J Psychiatry*. 1997;154:782-791.
21. Fox PT, Perlmutter JS, Raichle ME. A stereotactic method of anatomical localization for positron emission tomography. *J Comput Assist Tomogr*. 1985;9:141-153.
22. Miyazawa H, Osmont A, Petit-Taboué MC, et al. Determination of  $^{18}\text{F}$ -FDG brain kinetic constants in the anesthetized baboon. *J Neurosci Methods*. 1993;50:263-272.
23. Mazoyer BM, Huesman RH, Budinger TF, Knittel BL. Dynamic PET data analysis. *J Comput Assist Tomogr*. 1986;10:646-653.
24. Bendriem B, Soussaline F, Campagnolo R, Verrey B, Wajenberg P, Syrota A. A technique for the correction of scattered radiation in a PET system using time of flight information. *J Comput Assist Tomogr*. 1986;10:287-295.
25. Woods RP, Mazziotta JC, Cherry SR. MRI-PET registration with automated algorithm. *J Comput Assist Tomogr*. 1993;17:536-546.
26. Talairach J, Tournoux P. *Co-planar Stereotaxic Atlas of the Human Brain*. New York, NY: Thieme-Stratton; 1988.
27. Marchal G, Rioux P, Petit-Taboué MC, et al. Regional cerebral oxygen consumption, blood flow and blood volume in healthy human aging. *Arch Neurol*. 1992;49:1013-1020.
28. Logan J, Fowler JS, Volkow ND, et al. Graphical analysis of reversible radioligand binding from time-activity measurements applied to [ $^{11}\text{C}$ -methyl]-(-)-cocaine PET studies in human subjects. *J Cereb Blood Flow Metab*. 1990;10:740-747.

29. Petit-Taboué MC, Landeau B, Osmon A, Barré L, Baron JC. Determination of human cortical 5HT<sub>2</sub> receptor binding from <sup>18</sup>F-setoperone, kinetic PET data: comparison of different methods. *J Cereb Blood Flow Metab.* 1995;15(suppl 1):S641.
30. Seeman P, Niznik HB, Guan HC. Elevation of dopamine D2 receptors in schizophrenia is underestimated by radioactive raclopride. *Arch Gen Psychiatry.* 1990;47:1170–1172.
31. Bahn MM, Huang SC, Hawkins RA, et al. Models for in vivo kinetic interactions of dopamine D2-neuroreceptors and 3-(2'-<sup>18</sup>F fluoroethyl)siperone examined with positron emission tomography. *J Cereb Blood Flow Metab.* 1989;9:840–849.
32. Lassen NA, Bartenstein PA, Lammertsma AA, et al. Benzodiazepine receptor quantification in vivo in humans using <sup>11</sup>C-flumazenil and PET: application of the steady-state principle. *J Cereb Blood Flow Metab.* 1995;15:152–165.
33. Logan J, Wolf AP, Shiue CY, Foxler JS. Kinetic modeling of receptor-ligand binding applied to positron emission tomography studies with neuroleptic tracers. *J Neurochem.* 1987;48:73–87.
34. Frost JJ, Douglass KH, Mayberg HS, et al. Multicompartmental analysis of <sup>11</sup>C-carfentanil binding to opiate receptors in humans measured by positron emission tomography. *J Cereb Blood Flow Metab.* 1989;9:398–409.
35. Sadzot B, Price JC, Mayberg HS, et al. Quantification of human opiate receptor concentration and affinity using high and low specific activity <sup>11</sup>C-diprenorphine and positron emission tomography. *J Cereb Blood Flow Metab.* 1991;11:204–219.
36. Sadzot B, Lemare C, Maquet P, et al. Serotonin 5HT<sub>2</sub> receptor imaging in the human brain using positron emission tomography and a new radioligand, [<sup>18</sup>F]Altanserin: results in young normal controls. *J Cereb Blood Flow Metab.* 1995;15:787–797.
37. Schotte A, Maloteaux JM, Laduron PM. Characterization and regional distribution of serotonin S<sub>2</sub>-receptors in human brain. *Brain Res.* 1983;276:231–235.
38. Pazos A, Probst A, Palacios JM. Serotonin receptors in the human brain: IV. Autoradiographic mapping of serotonin S<sub>2</sub> receptors. *Neuroscience.* 1987;21:123–139.